Supplementary Table S1. siRNA

siRNA		Sequence
AR	Sense	5'- AAG AAG GCC AGU UGU AUG GAC -3'
	Antisense	5'-GUC CAU ACA ACU GGC CUU CUU -3'
MEN1 #1	Sense	5'- CCU CUA CCA CAA GGG CAU U -3'
	Antisense	5'- AAU GCC CUU GUG GUA GAG G -3'
MEN1 #2	Sense	5'- UCA CUU UCC AGA GUG AGA A -3'
	Antisense	5'- UUC UCA CUC UGG AAA GUG A -3'
SUV39H1 #1	Sense	5'- GGU GAA AUG GCG UGG AUA U -3'
	Antisense	5'- AUA UCC ACG CCA UUU CAC C -3'
SUV39H1 #2	Sense	5'- ACG CAU CAC UGU AGA GAA U -3'
	Antisense	5'- AUU CUC UAC AGU GAU GCG U -3'

Supplementary Table S2. RT-qPCR primer

Gene		Sequence
AR	Forward	5'- CAG TGG ATG GGC TGA AAA AT -3'
	Reverse	5'- AGG AGC TTG GTG AGC TGG TA -3'
ACTB	Forward	5'- GTC ACC AAC TGG GAC GAC AT -3'
	Reverse	5'- GAG GCG TAC AGG GAT AGC AC -3'
CAPG	Forward	5- CAG GTG GAG ATT GTC ACT GAT GG -3'
	Reverse	5'- CTG GGG ATT TGC CTT GTC AGC T -3'
GSN	Forward	5'- ATC TGC CAT CCT GAC TGC TCA G -3'
	Reverse	5'- CTT CCC ACC AAA CAG GCT CAT G -3'
HTRA1	Forward	5'- CAG ACG TGA TCT CAG GAG CGT A -3'
	Reverse	5'- TCG CTG ACA TCA TTG GCG GAG A-3'
LAMB3	Forward	5'- GTC ACA GAG CAG GAG GTG GCT -3'
	Reverse	5'- GCT TCT GTC AAG ACT CTC CAG G -3'
MEN1	Forward	5'- GTG GCC GAC CTG TCT ATC AT -3'
	Reverse	5'- GTG CCT GTG ATG AAG CTG AA -3'
SUV39H1	Forward	5'- GAT ATG ACC TCT GCA TCT TCC GC -3'
	Reverse	5'- GTA CAC GTC CTC CAC GTA GTC CAG -3'
TIMP2	Forward	5'- AAA GCG GTC AGT GAG AAG GA -3'
	Reverse	5'- CTT CTT TCC TCC AAC GTC CA -3'

Supplementary Table S3. TIMP2 ChIP qPCR primers

Promoter region		Sequence
TIMP2 #1	Forward	5'- CCT CTC CCT AGC TGG ACT GCA A -3'
	Reverse	5'- GTG GGC ACC CAC CCT GT -3'
TIMP2 #2	Forward	5'- GCC AGG CGC ACT TAA AAT TC -3'
	Reverse	5'- GGG TGG CCT ATT GAG AAA CTG A -3'
TIMP2 #3	Forward	5'- CAT TGG CCG CCA GCC AC -3'
	Reverse	5'- GCG CTG CCT TCT ACG GAT GT -3

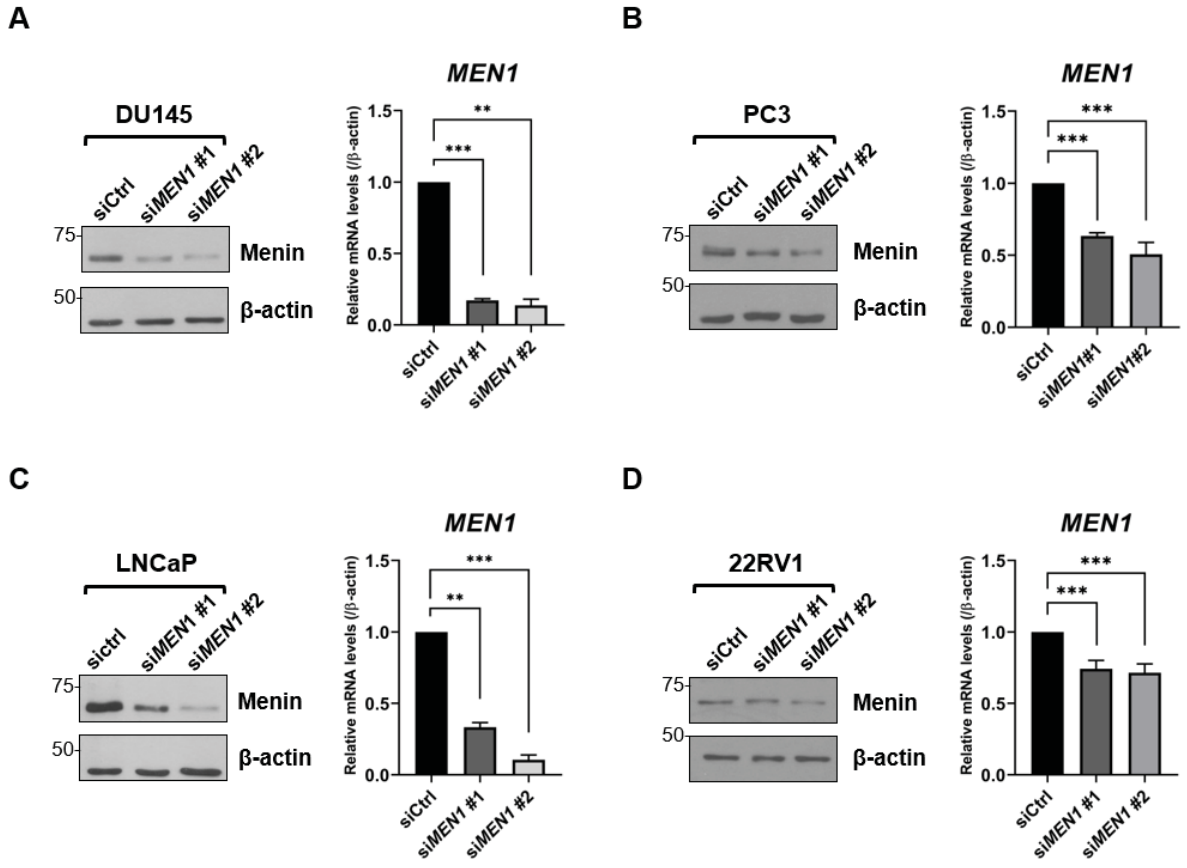

Supplementary Fig. S1. Depletion of menin with *MEN1*-specific siRNAs. Two independent siRNAs targeting the *MEN1* coding region were used for *MEN1* knockdown. In comparison, the siRNA targeting non-specific sequences was used as a control. Depletion of menin (67 KDa), as indicated by western blotting (WB, left) and RT-qPCR (right), is shown in DU145 (A), PC3 (B), LNCaP (C), and 22RV1 (D) cells. Beta-actin (49 kDa) was used as a loading control in WB. Beta-actin mRNA was used as an endogenous control for normalization in RT-qPCR. Bars show the mean mRNA level and SD. Statistical analyses were performed using an unpaired two-tailed *t*-test. ** $P < 0.01$; *** $P < 0.001$.

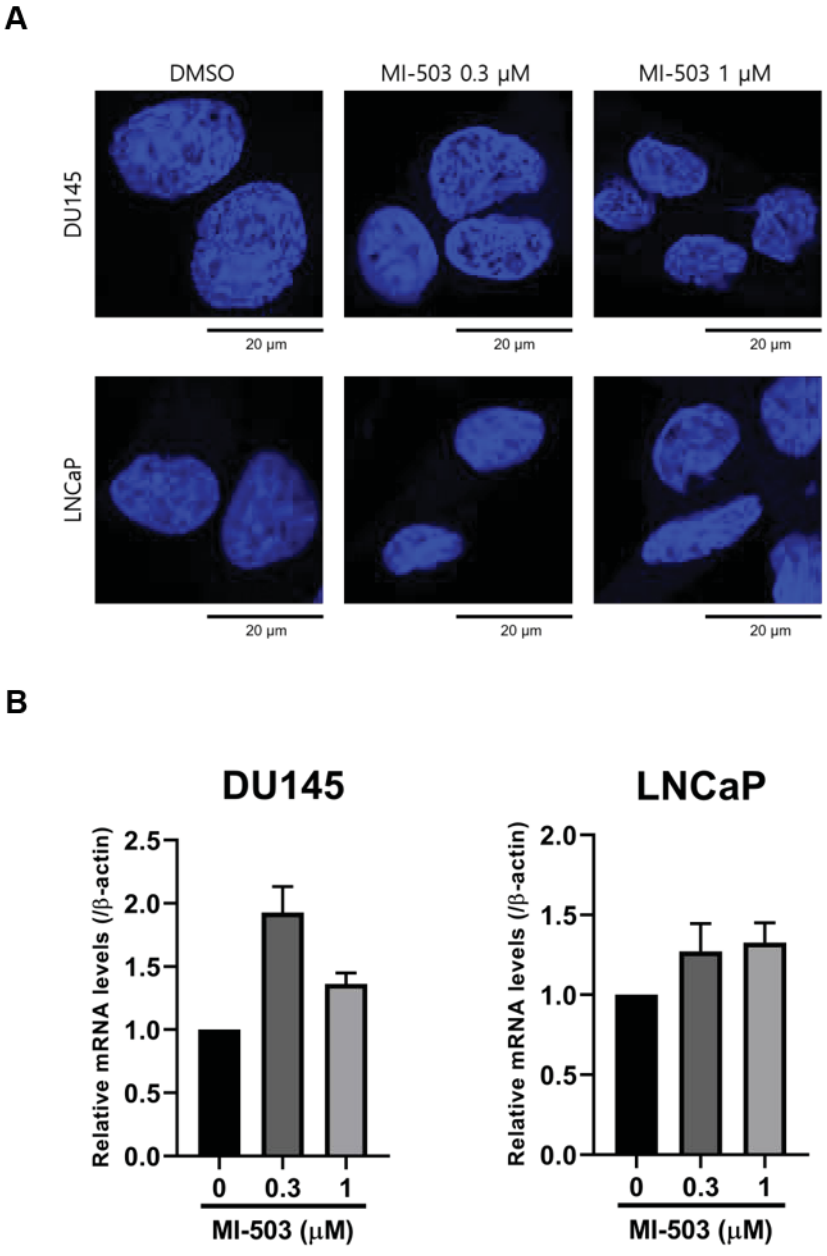

Supplementary Fig. S2. Treatment of prostate cancer cells with MI-503. (A) DAPI staining of MI-503-treated PCa cells. DU145 and LNCaP cells were treated with 0.3 or 1 μM of MI-503 for 48 h. (B) RT-qPCR for MI-503-treated DU145 (left) and LNCaP (right) cells. Bars show the mean mRNA level and SD. Beta-actin mRNA was used as an endogenous control for normalization in RT-qPCR.

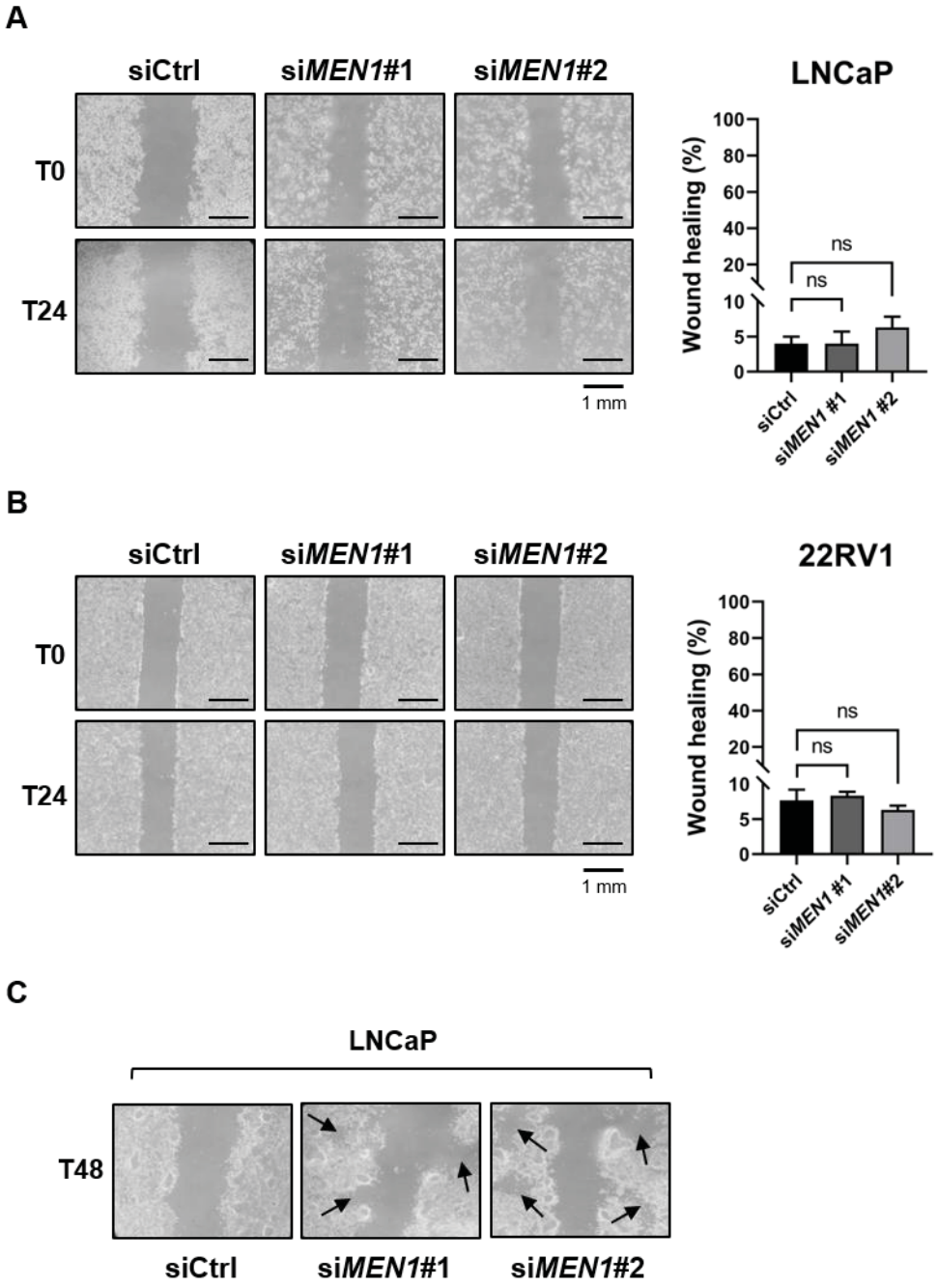

Supplementary Fig. S3. A wound healing assay with AR-positive PCa cells. (A and B) LNCaP (A) and 22RV1 (B) cells were scratched 48 h after siRNA transfection and the migration efficiency was analyzed 24 h after scratching. The percentage of wound healing was defined as the extent of relative wound closure (n = 3). Scale bar = 1 mm. ns, not significant. (C) Cell images of LNCaP acquired 48 h after scratch. The arrows indicate where significant populations of cells were dead and detached (n = 3).

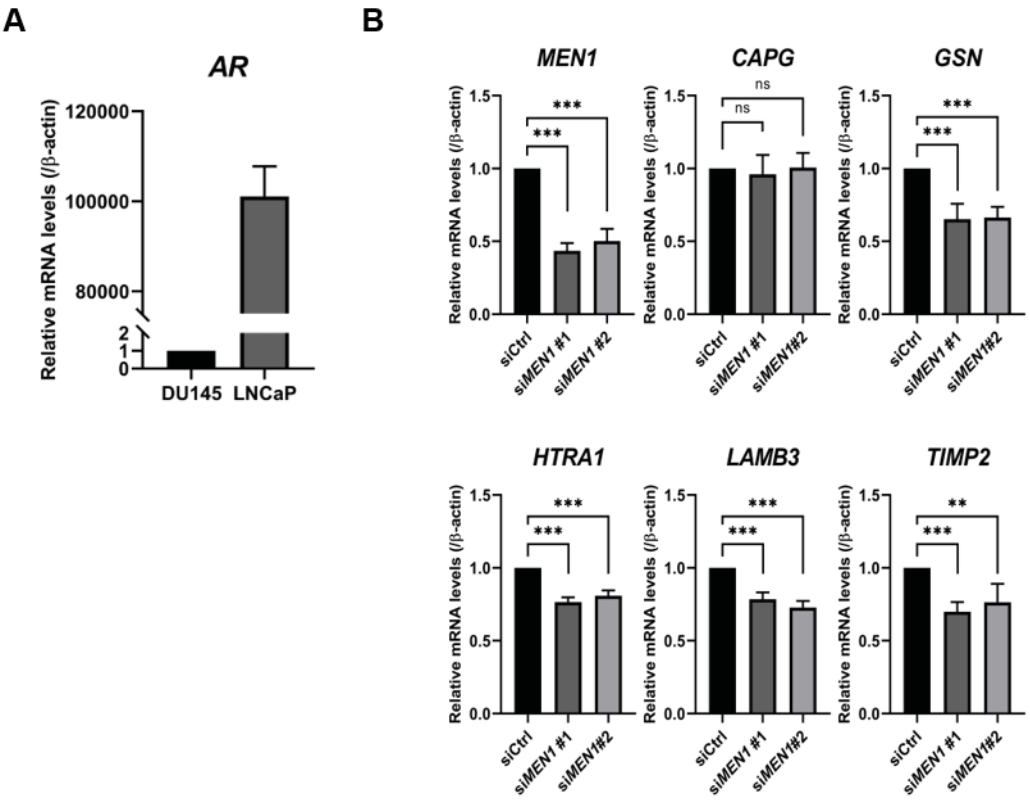

Supplementary Fig. S4. The relative mRNA analysis of PCa cells. (A) Total RNAs from DU145 and LNCaP cells were isolated, and the *AR* and *ACTB* (control) mRNA levels were analyzed by RT-qPCR, using gene-specific primers. (B) PC3 cells were treated with a control or *MEN1*-specific siRNAs. Bars show the mean mRNA level and SD. Statistical analyses were performed using an unpaired two-tailed *t*-test. $^{**}P < 0.01$; $^{***}P < 0.001$; ns, not significant.

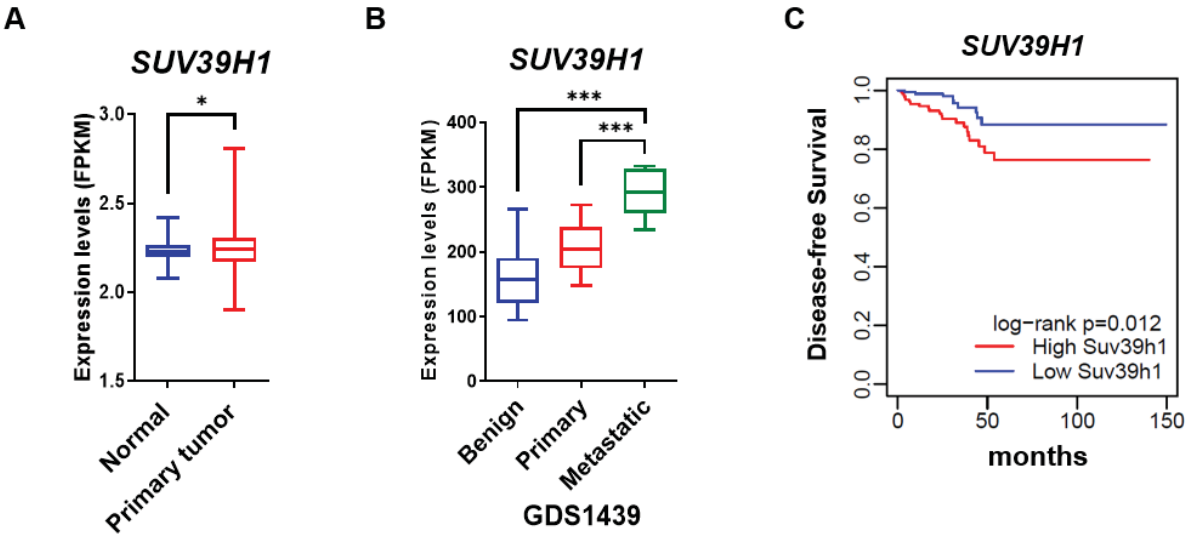

Supplementary Fig. S5. *SUV39H1* is potentially associated with metastasis of prostate cancer. (A) The relative mRNA expression in the TCGA cohort between normal and cancer tissues (normal = 52, primary tumor = 497). (B) Analysis of *SUV39H1* expression from the GEO profiles. Analysis of GEO dataset (GDS1439) showed a statistically significant difference between benign and cancer tissues (benign n = 6, primary tumor n = 7, and metastatic n = 6). (C) Kaplan-Meier disease-free survival analysis of prostate adenocarcinoma patients with high (n = 156, red line) and low (n = 176, blue line) *SUV39H1*. *P* values were determined using the log-rank test.

Full scan (uncropped) western blot images

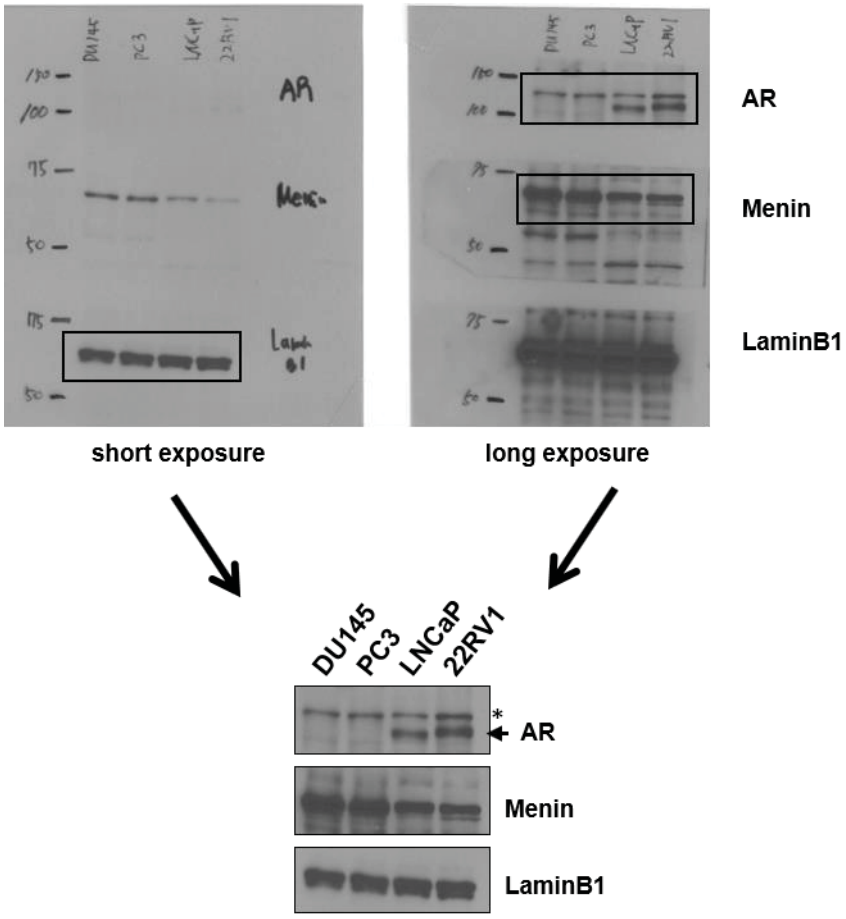

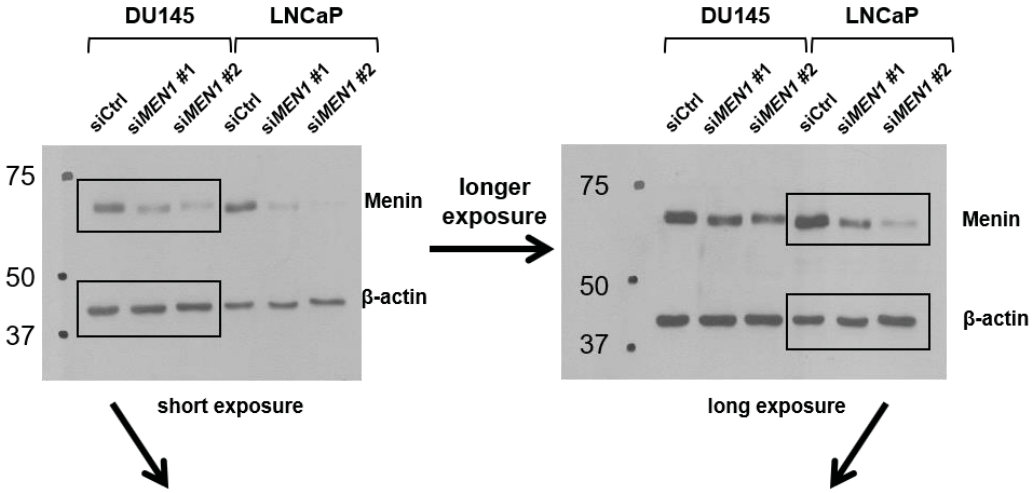

Supplementary Figure S1A

Supplementary Figure S1C

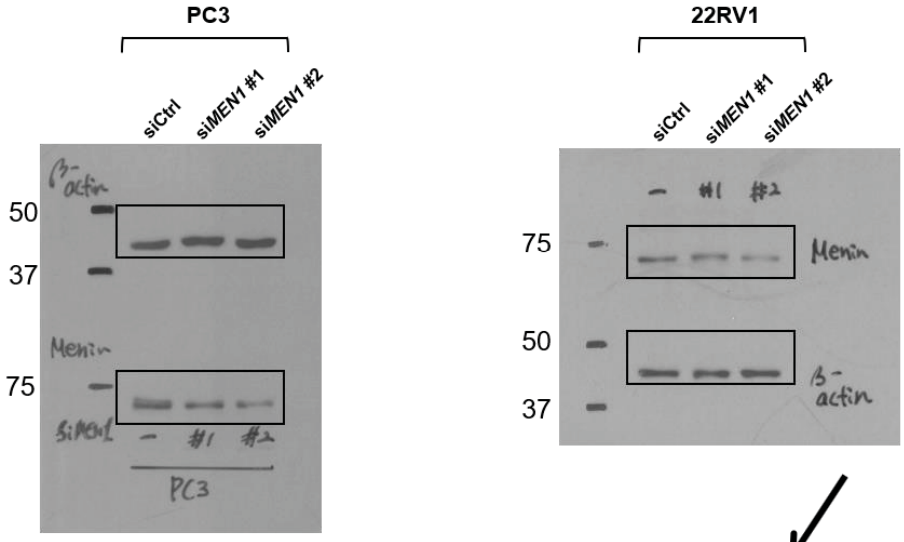

Supplementary Figure S1B

Supplementary Figure S1D

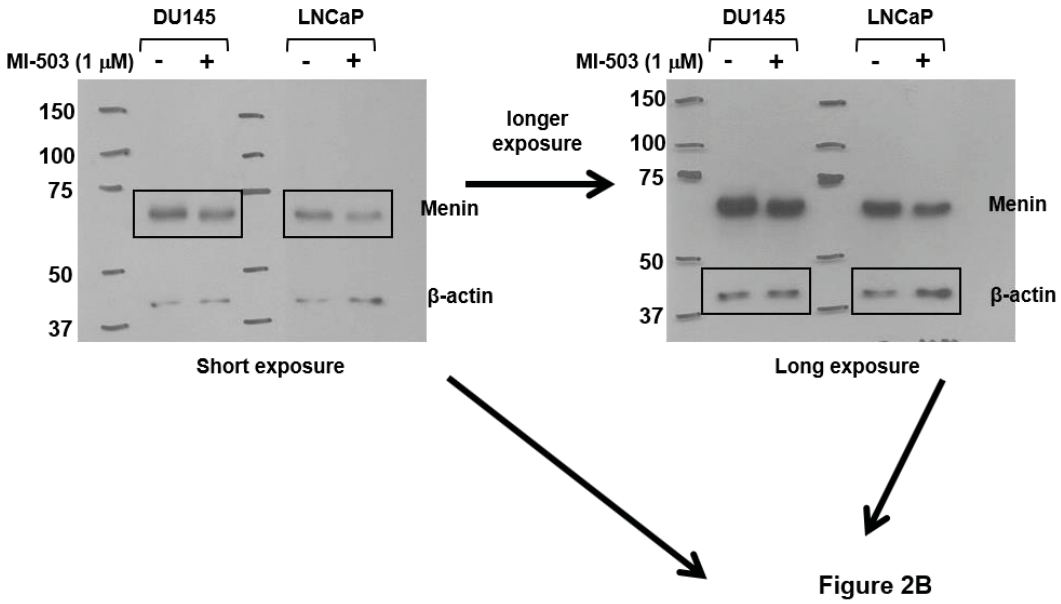

Figure 2B

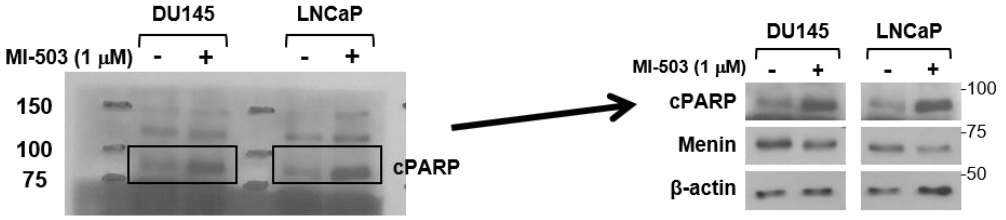

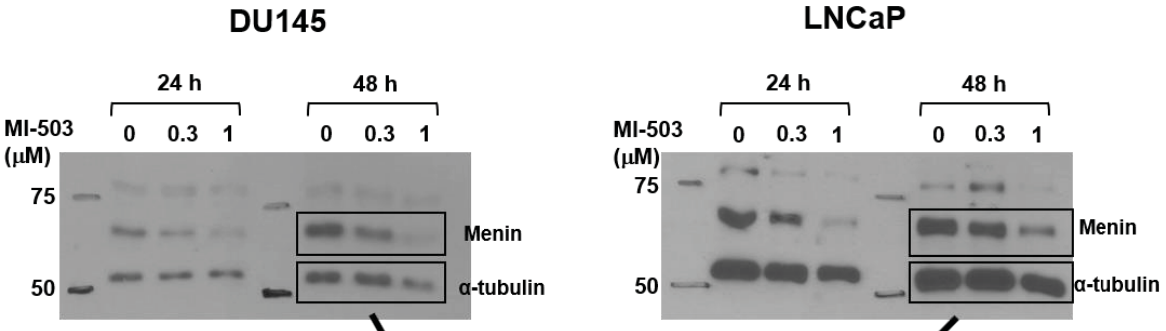

Figure 2D